

# Theoretical Studies of Structural Effects on the Mechanism of Acyl-Transfer Reactions<sup>1</sup>

Ikchoon Lee,\* Doyoung Lee, and Chang Kon Kim

Department of Chemistry, Inha University, Incheon 402-751, Korea

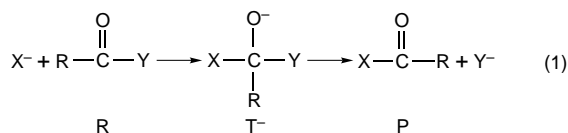
Received: April 18, 1996; In Final Form: August 2, 1996<sup>⊗</sup>

Potential energy profiles have been determined for the two series of reactions: (i)  $X^- + \text{HCOY}$ , where  $X = Y = \text{H, F, or Cl}$ , and (ii)  $X^- + \text{RCOX}$ , where  $X = \text{F or Cl}$  and  $R = \text{SiH}_3, \text{CH}_3, \text{H, CN, or NO}_2$ . Energies of all stationary points, including reactants, ion–dipole complexes, stable adducts, transition states, and products, were evaluated at the Hartree–Fock (HF) and the second-order Møller–Plesset (MP2) correlation levels with the 6-311++G\*\* for reaction series i and with the 6-31+G\* basis set for reaction series ii. The results predict that acyl-transfer reactions can proceed through single-well, double-well, and triple-well energy profiles in the gas phase depending on the nucleophile,  $X^-$ , nucleofuge  $Y^-$ , and acyl group R. Factors that favor the single-well or triple-well profile with a stable tetrahedral adduct are (a) stronger bond formation of the C–X or C–Y bond, (b) stronger nucleophilicity of  $X^-$  and poorer leaving ability of the nucleofuge,  $Y^-$ , (c) wide energy gap between the two antibonding MOs,  $\pi^*_{\text{C=O}}$  and  $\sigma^*_{\text{C-X}}$ , and (d) strong electron acceptor acyl group, R. Whenever gas-phase experimental results are available, good agreements were obtained with our MP2 predictions.

## Introduction

Nucleophilic carbonyl addition reactions are one of the fundamental classes of reactions in organic chemistry and biochemistry. In view of their importance in biochemical processes and synthetic utility, carbonyl addition reactions have been extensively studied both in solution and in the gas phase. Early experimental results in solution suggested that acyl-transfer reactions occur through a stepwise mechanism involving a tetrahedral addition intermediate.<sup>2</sup> Subsequent studies, however, indicated that the reaction can also occur through a concerted, one-step mechanism with a single tetrahedral transition state (TS) and no addition intermediate.<sup>3</sup>

Recent developments in gas-phase ion chemistry have enabled us to observe the gas-phase, solvent-free reactions revealing the intrinsic reactivities of the carbonyl addition reactions which are determined solely by the electronic and structural nature of the reactants.<sup>4</sup> Brauman and co-workers<sup>4g,o,p</sup> reported their ion cyclotron resonance results on displacement reactions of nucleophiles including halide ions with acyl halides in the gas phase. They interpreted their kinetic data in terms of double-well energy surfaces with the tetrahedral structure at the saddle point and the two ion–dipole complexes at the energy minima. This proposal has since provoked theoreticians to theoretically investigate the true nature of the tetrahedral adduct,  $T^-$ , using relatively simple acyl-transfer processes.

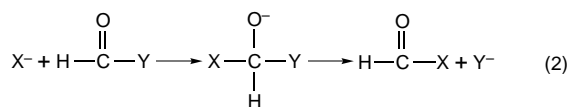


Conflicting theoretical findings have been reported as to the nature, i.e., TS or intermediate, of the tetrahedral adduct,  $T^-$ , depending on the systems employed in the theoretical investigations. Burgi et al.<sup>5</sup> reported the results of SCF-LCGO-MO calculations that hydride addition to formaldehyde ( $R = X = Y = \text{H}$ ) proceeds to form the tetrahedral intermediate, which was 48 kcal/mol below the reactants, with no barrier. This is

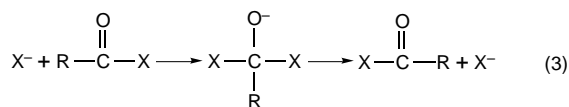
in agreement with the gas-phase experimental results of Bohme et al.<sup>6</sup> that in the gas-phase reactions of  $\text{H}^-$ ,  $\text{HO}^-$ , and  $\text{CH}_3\text{O}^-$  with  $\text{H}_2\text{C}=\text{O}$  stable tetrahedral adducts are produced. On the other hand, *ab initio* calculations of Madura and Jorgensen<sup>7</sup> at the 6-31+G\* level on the energy profile for the nucleophilic addition of hydroxide ion to  $\text{H}_2\text{C}=\text{O}$  showed that the reaction proceeds in the gas phase by the conversion of reactants to the tetrahedral intermediate (exothermic by 35 kcal/mol) and via an ion–dipole complex in the later stage.

In contrast, however, when the leaving ability of group Y in (1) is increased to  $Y = \text{Cl}$ , double-well energy surfaces are obtained for both  $\text{HCOCl}$  and  $\text{CH}_3\text{COCl}$  with the attacking anion of  $\text{Cl}^-$  at the MP2/6-31+G\*\*/3-21G level.<sup>8</sup> For these reactions the tetrahedral adduct is the TS and ion–dipole complexes are at the energy minima. Similarly for the reactions of  $\text{CH}_3\text{COCl} + \text{F}^-$  and  $\text{CH}_3\text{COF} + \text{Cl}^-$ , double-well energy surfaces are obtained with the 4-31G+p+p' basis set.<sup>9</sup>

To extend our understanding of the factors that are important in determining the nature of the tetrahedral adduct, we have carried out *ab initio* MO calculations on the two reaction series in which the nucleophile and leaving group are varied, (2), and the acyl group is varied, (3).



where  $X, Y = \text{H, F, or Cl}$ .



where  $R = \text{SiH}_3, \text{CH}_3, \text{H, CN, or NO}_2$  and  $X = \text{F or Cl}$ .

## Calculation

The calculations were carried out with the Gaussian 92 series of programs.<sup>10</sup> Geometries and the gas-phase potential energy surfaces were determined at the HF/6-311++G\*\* (HF/6-311++G\*\*//HF/6-311++G\*\*) and MP2/6-311++G\*\* (MP2/

<sup>⊗</sup> Abstract published in *Advance ACS Abstracts*, January 1, 1997.

**TABLE 1: Total Energies (hartrees) and Relative Energies,  $\Delta E$  (kcal/mol), of Stationary Points on the  $X^- + R-CO-Y$  Potential Energy Surface Calculated with the MP2/6-311++G\*\* Basis Set**

no.	X	Y	reactants	RC	TS1	T <sup>-</sup>	TS2	PC	P	$\Delta E^a$	$\sigma^*$ attack TS
(i)	H	H	-114.747 38 (-114.770 44) <sup>c</sup>	-114.764 73 (-114.787 01)	-114.764 48(1i) <sup>b</sup> (-114.786 86) (1i)	-114.820 33 (-114.836 73)	-114.764 48(1i) (-114.786 86) (1i)	-114.764 73 (-114.787 01)	-114.747 38 (-114.770 44)	-45.78 (-41.60)	-114.638 61(2i) <sup>d</sup> (79.0) <sup>e</sup>
(ii)	H	F	-213.857 97	-213.886 22	-213.875 7(1i)	-213.952 56	-213.946 15(1i)	-213.948 83	-214.920 46	-59.36	-213.824 93(2i) <sup>d</sup> (32.0) <sup>e</sup>
(iii)	H	Cl	-573.823 28					-573.963 88	-573.945 34		
(iv)	F	F	-313.031 05			-313.081 78			-313.031 05	-31.83	
(v)	F	Cl	-627.996 35					-673.082 87	-673.055 93		
(vi)	Cl	Cl	-1033.021 24	-1033.050 19	-1033.036 53(1i)	-1033.036 53	-1033.036 53(1i)	-1033.050 19	-1031.021 24	9.59	-1033.008 47(2i) <sup>d</sup> (17.6) <sup>e</sup>

<sup>a</sup>  $\Delta E = E(T^-) - E(\text{Reactants})$ . <sup>b</sup> Only one negative eigenvalue of the harmonic frequency is confirmed, (1i). <sup>c</sup> Values in parentheses are fully optimized at QCISD/6-311++G\*\* level. <sup>d</sup> Two negative eigenvalues of the harmonic frequency are obtained, (2i). <sup>e</sup> The  $\sigma^*$  attack TS(2i) is higher by the amount (in kcal mol<sup>-1</sup>) shown in the parentheses than  $\pi^*(\text{TS1})$  attack TS.

6-311++G\*\*//MP2/6-311++G\*\*) levels for reaction series 2 and at the HF/6-31+G\* (HF/6-31+G\*/HF/6-31+G\*) and MP2/6-31+G\* (MP2/6-31+G\*/MP2/6-31+G\*) levels for reaction series 3. For R = CH<sub>3</sub>, H, and CN, MP4 level calculations were also carried out (MP4/6-31+G\*/MP2/6-31+G\*). In the discussion we will refer to the two levels simply as the HF and MP2 or MP4. For the reaction system of H<sup>-</sup> + HCOH, we have done similar calculations at the QCISD/6-311++G\*\* level of theory. All geometries of the reactants, complexes, transition structures, and products were fully optimized. The stationary points including transition structures were fully characterized through harmonic vibrational frequency analysis.<sup>12</sup>

## Results and Discussion

**(I) Nucleophile and Leaving Group Effect.** The potential energy profiles for acyl-transfer reactions belonging to reaction series 2 have been determined with the 6-311++G\*\* basis sets at the HF and MP2 levels. The energetics are summarized in Table 1. In the following, the results are presented and discussed for each reaction.



The salient features of the HF and MP2 energy surfaces are shown in Figure 1. Formation of the tetrahedral adduct is very much favorable energetically with the hydride ion. Since this reaction is an identity exchange process, the potential surfaces are a symmetric triple-well type. The central well, which represents a stable tetrahedral intermediate, is deeper at the MP2 (-45.8 kcal/mol) than the HF (-33.9 kcal/mol) level. In contrast the energy barrier to the central well from the ion-dipole complex is marginal at the MP2 level (0.2 kcal/mol) in contrast to a somewhat higher barrier at the HF level (5.5 kcal/mol). Thus at the MP2 level of theory the stable intermediate is formed almost directly from the reactants and the potential energy profile is practically a single-well type. This can be ascribed to strong bond formation of C-H coupled with high nucleophilicity and low nucleofugacity of the hydride ion. Our results are consistent with the tetrahedral adduct observed in the gas phase experimentally,<sup>6</sup> which has been confirmed also by calculation at a much lower level of *ab initio* theory.<sup>5</sup> The ion-dipole  $\pi$  complex is formed by electrostatic interaction.<sup>8,9,13</sup> This type of cluster is experimentally found to be typically bound by 10–12 kcal/mol,<sup>13</sup> as our results indicate. The reaction is experimentally known to proceed through a stable tetrahedral intermediate, which is exothermic by more than 10–12 kcal/mol,<sup>14</sup> as our *ab initio* result (35.1 kcal/mol) shows. Our results at the QCISD/6-311++G\*\* level also gave an essentially similar energy profile as that of MP2 with a slightly deeper central well depth (by 4.18 kcal mol<sup>-1</sup>). Our MP2

structures of the ion-dipole complex and the adduct are given in Figure 2.



For this reaction, the potential energy profiles (Figure 1) are skew triple-well type at both the HF and MP2 levels due to greater basicity (nucleophilicity) of the hydride than the fluoride anion. The two ion-dipole  $\pi$  complexes, HCOF $\cdots$ H<sup>-</sup> and HCOH $\cdots$ F<sup>-</sup>, are of similar strength with 17.7 and 17.8 kcal/mol at the MP2 level, respectively. The central well corresponding to the adduct, (H<sub>2</sub>COF)<sup>-</sup>, is deeper (47.0 and 59.3 kcal/mol at the HF and MP2 levels), for the forward process, but is shallower (16.9 and 20.1 kcal/mol at the HF and MP2 levels) than the identity hydride exchange (i) above. This indicates clearly much poorer leaving ability of the hydride than fluoride anion. The energy barrier to the tetrahedral adduct formation is greater for the forward process (6.5 kcal/mol at the MP2 level) than that for the reverse reaction (1.7 kcal/mol at the MP2 level). Nevertheless the reaction can proceed in the forward direction and the reverse reaction will be a quite difficult process. This is also ascribable to the higher nucleophilicity and lower leaving ability of H<sup>-</sup> compared to F<sup>-</sup>. The structures of the ion-dipole complexes and the TSs corresponding to the intermediate barriers are shown in Figure 2.



For this reaction, the potential energy profile (Figure 1) is radically different depending on the level of theory used: it is a double-well type with the HF, whereas it is a single-well type at the MP2 level. The central well corresponding to the stable tetrahedral adduct is very deep in the forward process (80.2 and 88.2 kcal/mol at the HF and MP2 levels, respectively) but is shallow in the reverse direction (11.3 and 11.6 kcal/mol at the HF and MP2 levels, respectively). This is again an indication of large differences in the nucleophilicity and leaving abilities of the two anions, H<sup>-</sup> and Cl<sup>-</sup>. In the gas phase, therefore, the forward reaction will be facile, whereas the reverse reaction should be practically prohibited. In the potential energy surface obtained at the HF level, a shallow minimum corresponding to the ion-dipole complex, H<sup>-</sup> $\cdots$ HCOCl, is noted. Any such shallow minimum corresponding to HCOH $\cdots$ Cl<sup>-</sup> must have been swamped by the extremely deep central well.<sup>7,9</sup> Similar behaviors were found by Madura and Jorgensen<sup>7</sup> for the OH<sup>-</sup> + HCOH reaction at the 6-31+G\* level and also by Wu et al.<sup>15</sup> for the <sup>-</sup>OCH<sub>3</sub> + HCOH reaction at the 3-21G level. Our results of a single-well type potential energy surface at the MP2 level indicate clearly that such a shallow minimum is only an artifact of the neglect of electron correlation effect. The single-well potential energy surface is therefore ascribed to the

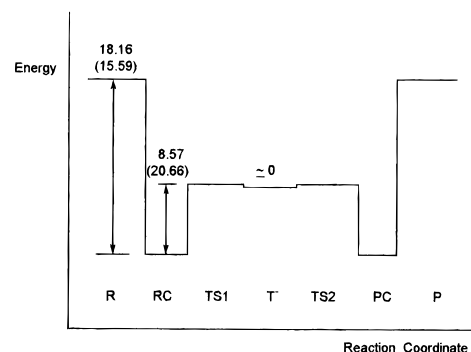
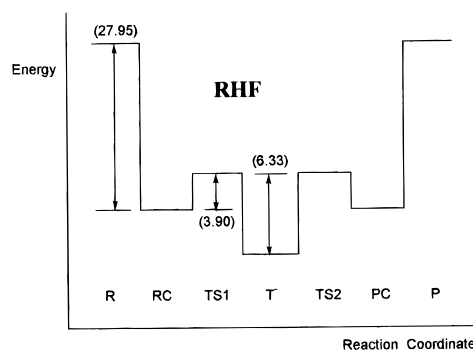
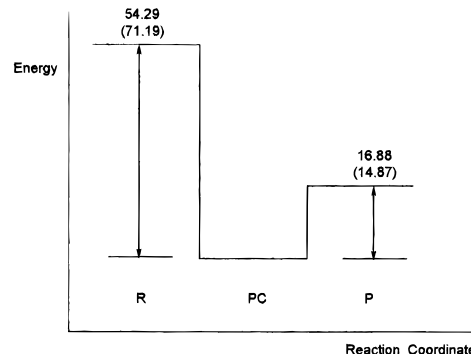
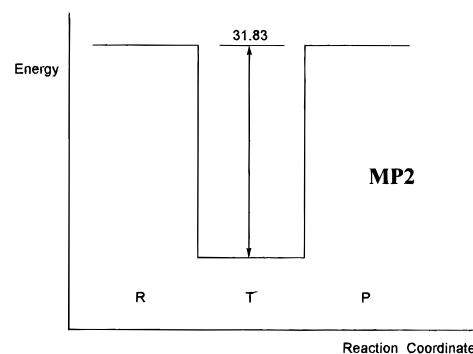
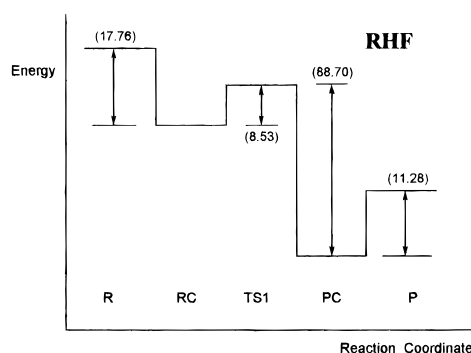
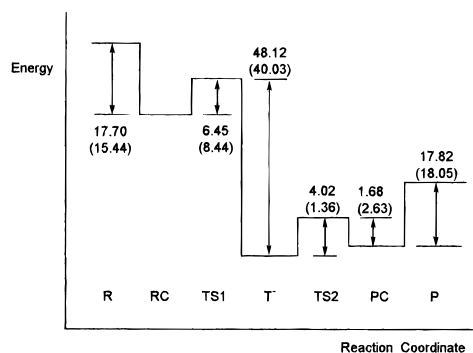
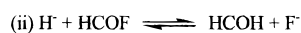
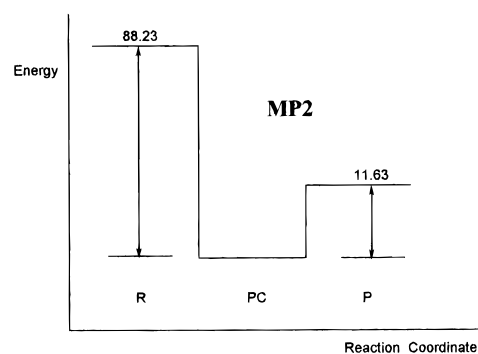
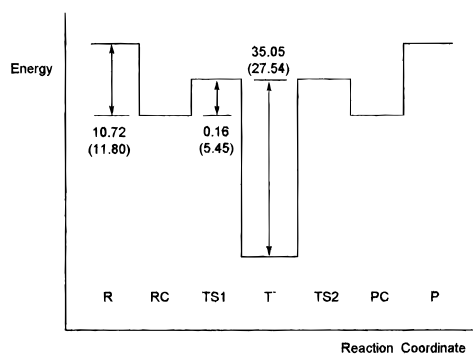


**Figure 1.** Potential energy profiles (kcal/mol) for the reaction of  $\text{X}^- + \text{HCOY}$  with the MP2/6-311++G\*\* method. The RHF values are given in parentheses. Geometries of R, RC, TS1, and T<sup>-</sup> are shown in Figure 2.

extremely large exothermic formation of an adduct. The well-depth for this reaction is in fact the largest among the reaction series studied in this work. The structure of the adduct is shown in Figure 2.



For this identity exchange reaction, the HF potential energy profile is a triple well, whereas the MP2 energy profile is a single-well type. The MP2 well-depth is relatively small (31.8

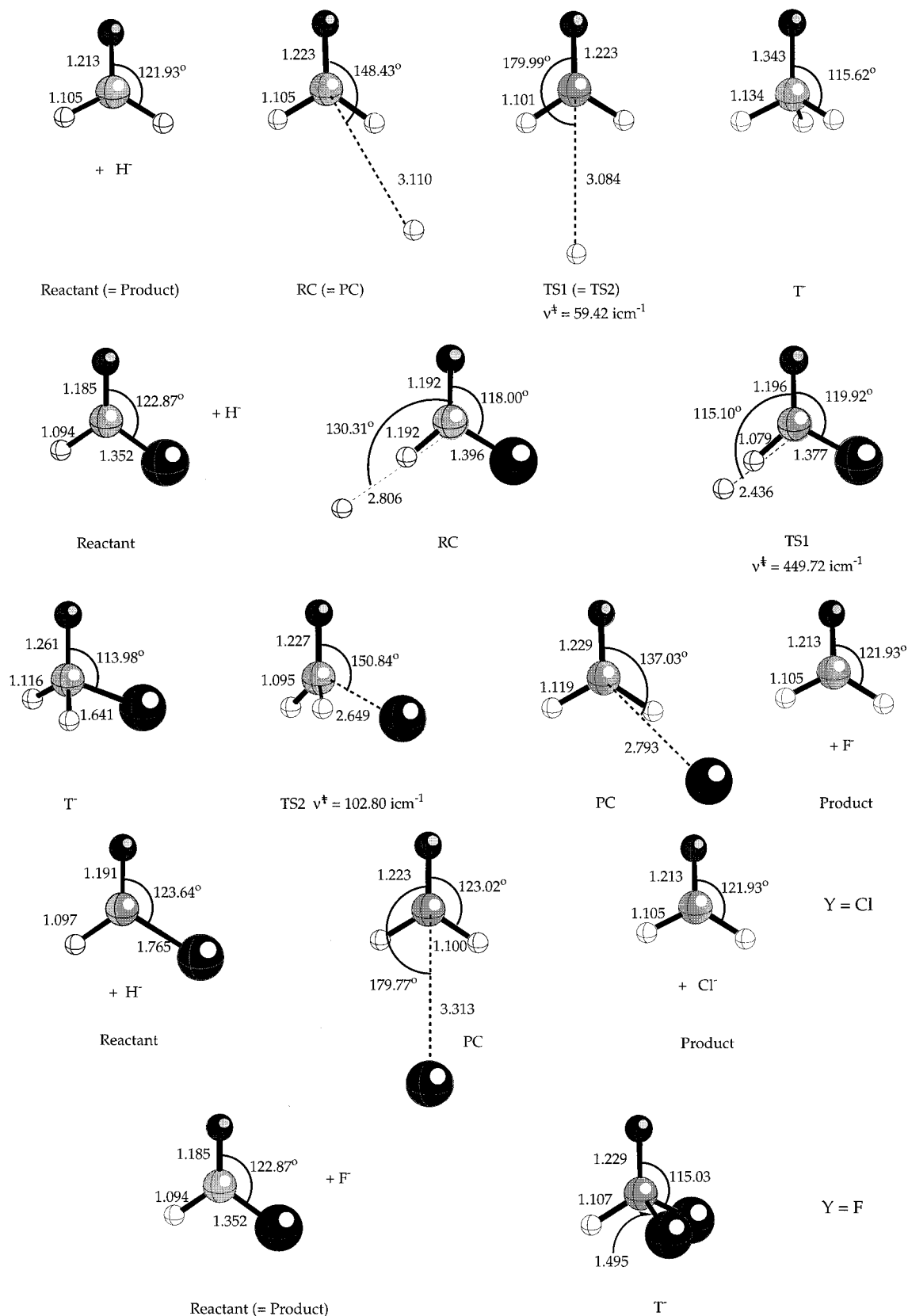


**Figure 2.** MP2 optimized structures of stationary point species for the reactions of  $\text{H}^- + \text{HCOY}$ . Distances are in Angstroms, and bond angles are in degrees. Top:  $\text{Y} = \text{H}$ . Middle:  $\text{Y} = \text{F}$ . Bottom:  $\text{Y} = \text{C}$ .

kcal/mol) compared to the other processes discussed above. The  $\text{F}^-$  ion is a basic, strong nucleophile but is a poor leaving group. The presence of the two strong electronegative F atoms within the tetrahedral adduct,  $\text{HF}_2\text{CO}^-$ , could contribute to its relatively low stability. Here again the ion-dipole complexes in the triple-well energy profile obtained at the HF level must be an artifact of the neglect of electron correlation effect; inclusion of electron

correlation results in the instability of the ion-dipole  $\pi$  complexes which are swamped by the more exothermic adduct formation, leading to their disappearance.<sup>7,9</sup> This is similar to the disappearance of ion-dipole complexes on the MP2 potential surface in the  $\text{H}^- + \text{HCOCl}$  process, (iii), above.



The forward reaction is characterized by a strong nucleophile,  $F^-$ , coupled with a relatively strong nucleofuge,  $Cl^-$ . The HF as well as MP2 energy profile (Figure 1) is a skew single-well type, as expected from the similar MP2 potential surface for the reaction of  $H^-$  and  $HCOCl$ . Despite the stronger bond of  $F-C$  (116 kcal/mol)<sup>16</sup> than  $H-C$  (99 kcal/mol),<sup>16</sup> the adduct well is much deeper for the  $H^- + HCOCl$  process (88.2 kcal/mol by MP2) than  $F^- + HCOCl$  (54.3 kcal/mol by MP2). This indicates that the bond strength of the bond formed in the adduct is not the only factor determining the stability of the adduct. For example, the electronegativity of the radical and anionic form is much greater for  $F$  (3.40 eV)<sup>17</sup> than  $H$  (0.74 eV),<sup>17</sup> but the latter should be more polarizable. These two factors could contribute to the more stable adduct formation with  $X = H$  rather than with  $X = F$ . Since the well-depth for the reverse process is small (16.9 kcal/mol by MP2), the forward reaction can be facile, but the reverse reaction is a very difficult process. The structure of the MP2 adduct is shown in Figure 2.



The potential energy profile (Figure 1) for this identity exchange reaction has a typical double-well structure at both the HF and MP2 levels. The central barrier is however much lower at the MP2 level (8.6 vs 20.7 kcal/mol). It is interesting to note here that improvement of basis sets used in the computation in general lowers the central (intrinsic) barrier,  $\Delta E_0^\ddagger$ ; the  $\Delta E_0^\ddagger$  values are 23.4 and 20.7 kcal/mol at the HF/6-31+G\*\*/HF/3-21+G<sup>8</sup> and HF/6-311++G\*\*//6-311++G\*\* levels, respectively, and 11.7, 15.3, and 8.6 kcal/mol at the MP2/6-31+G\*\*//3-21+G,<sup>8</sup> MP3/MP2/6-31+G\*\*//3-21+G,<sup>8</sup> and MP2/6-311++G\*\*//MP2/6-311++G\*\* levels, respectively. In both cases, our values (last) are the lowest due to the much better basis sets used.

The double-well structure is consistent with the gas-phase experimental results of Brauman<sup>4b</sup> and co-workers for  $CH_3COCl + Cl^-$ . The lower level *ab initio* calculations by Yamabe et al.<sup>9</sup> on  $CH_3COCl + Cl^-$  and by Blake et al.<sup>8</sup> on  $HCOCl + Cl^-$  and  $CH_3COCl + Cl^-$  have also indicated the double-well type potential surface with the tetrahedral transition state. The two energy minima correspond to the ion-dipole  $\pi$  complexes reported by the previous workers.<sup>8,9</sup>

Among the reactions studied in the present work, this is the only one that does not proceed through a stable tetrahedral adduct. The chloride ion has the lowest basicity (nucleophilicity) but also the highest leaving ability among the anion nucleophiles studied in this work,  $H^-$ ,  $F^-$ , and  $Cl^-$ . Since the  $C-Cl$  bond is relatively weak, the energy accompanying deformation and the bond scission in the substrate requires more energy than that released in the bond formation, and hence the barrier is introduced.

The electronegativity of the radical and anionic forms of the nucleophile (or nucleofuge) has been shown to increase in the order  $H^- < F^- < Cl^-$  (0.74, 3.40, and 3.62 eV, respectively),<sup>17</sup> and hence the nucleofugacity is expected to increase in the same order. With the worst leaving group,  $H^-$ , the tetrahedral adduct can be relatively stable (exothermic by 45.8 kcal/mol at the MP2 level), but for the much better leaving group,  $Cl^-$ , the adduct becomes unstable and a direct concerted displacement mechanism prevails. In between the two rather extreme cases, there is an intermediate case of  $F^-$ , which can form an adduct of rather low stability (exothermic by 31.8 kcal/mol at the MP2 level). The situation is reminiscent of the different mechanisms found for the identity  $S_N2'$  reactions of  $X^- + CH_2=CH-CH_2X$  with  $X = H, F, \text{ and } Cl$ .<sup>18</sup> The reaction was found to proceed by a stepwise  $S_N2'$  mechanism in which the breakdown of a stable adduct is rate-limiting for  $X = H$ , whereas the concerted

**TABLE 2: Energy Gaps,  $\Delta\epsilon$  (eV), between Two Antibonding Orbitals,  $\pi^*_{C=O}$  and  $\sigma^*_{C-X}$  (hartree), with the 6-31+G\* Basis Sets<sup>a</sup> for  $R-CO-X$  (1 hartree = 27.21 eV)**

R	X	antibonding orbital (hartree)	$\Delta\epsilon(\sigma^* - \pi^*)$
SiH <sub>3</sub>	F	$\sigma^*_{C-X}$	0.4177
		$\pi^*_{C=O}$	0.1756
CH <sub>3</sub>	Cl	$\sigma^*_{C-X}$	0.2556
		$\pi^*_{C=O}$	0.1533
	F	$\sigma^*_{C-X}$	0.4445
		$\pi^*_{C=O}$	0.1858
H	Cl	$\sigma^*_{C-X}$	0.2846
		$\pi^*_{C=O}$	0.1653
	F	$\sigma^*_{C-X}$	0.4539
		$\pi^*_{C=O}$	0.1676
CN	Cl	$\sigma^*_{C-X}$	0.3021
		$\pi^*_{C=O}$	0.1471
	F	$\sigma^*_{C-X}$	0.4285
		$\pi^*_{C=O}$	0.1267
NO <sub>2</sub>	Cl	$\sigma^*_{C-X}$	0.2802
		$\pi^*_{C=O}$	0.1104
	F	$\sigma^*_{C-X}$	0.4397
		$\pi^*_{C=O}$	0.1130
	Cl	$\sigma^*_{C-X}$	0.2929
		$\pi^*_{C=O}$	0.1018

<sup>a</sup> Calculated using the NBO method.

$S_N2$  reaction was found to be the most favored for  $X = Cl$ . For  $X = F$  all three pathways, i.e., anti- $S_N2'$ , syn- $S_N2'$ , and  $S_N2$ , were competitive.

Besides the strength of bonds that are formed and broken in the TS, the MO level gap between  $\sigma^*_{C-X}$  and  $\pi^*_{C=O}$  constitutes another factor that determines whether the acyl-transfer reactions proceed through a stable tetrahedral adduct or through a tetrahedral TS. The importance of the  $\sigma^*-\pi^*$  orbital mixing for the nucleophilic displacement on the unsaturated carbon has been discussed in detail by Yamabe et al.<sup>9b</sup> When the nucleophile ( $Cl^-$ ) approaches the carbon atom of the  $\pi^*_{C=O}$  MO, the  $\pi$  complex is formed, which induces bending of the  $C-Cl$  bond.<sup>9</sup> This deformation in turn lowers the LUMO and the orbital mixing between  $\sigma^*_{C-Cl}$  and  $\pi^*_{C=O}$  MOs. If the two MOs are separated by a large energy gap, the mixing effect will be small and the approaching nucleophile forms a tetrahedral adduct through  $\pi$  approach. However when the energy gap is small enough to induce sufficient mixing of the  $\sigma^*_{C-Cl}$  and  $\pi^*_{C=O}$  MOs, the  $\sigma^*_{C-Cl}$  MO becomes a main component of the LUMO so that charge transfer from the nucleophile leads to the weakening of the  $C-Cl$  bond. Thus the tetrahedral species becomes a TS, but not a stable adduct. Thus the narrower the energy gap between  $\pi^*_{C=O}$  and  $\sigma^*_{C-Cl}$ , the greater the possibility of the tetrahedral species becoming a TS rather than a stable adduct. For example, the energy gaps between the two antibonding MOs,  $\Delta\epsilon(\sigma^*-\pi^*)$ , in Table 2, for  $F^- + HCOF$  and  $Cl^- + HCOCl$  are 7.79 and 4.22 hartrees, respectively. The gap for  $Cl^-$  reactions is only half of that for the reaction of  $F^-$ , so that  $\sigma^*-\pi^*$  mixing will be much efficient for  $Cl^-$  reaction. This is why we obtained a tetrahedral adduct for the former,  $F^-$ , but a tetrahedral TS for the latter,  $Cl^-$ . The structures of the ion-molecule complex and the TS are shown in Figure 2. The "linear" channel with a trigonal-bipyramidal TS discussed by Yamabe et al.<sup>19</sup> for the reaction system of  $Cl^- + PhCOCl$  has been also considered in our work for the two reaction systems (Table 1). However in both cases that we investigated ( $H^- + HCOH$  and  $Cl^- + HCOCl$ ) we obtained two negative eigenvalues, so that we failed to identify the true TSs.

Recently, Radom and co-workers reported<sup>20</sup> a G2 type calculation on the  $Cl^- + CH_2=CHCl$  reaction. Their results indicated that, in the gas phase, in-plane  $\sigma$  type  $S_N2$  substitution with inversion at an unactivated  $sp^2$  carbon is energetically favored to the out-of-plane  $\pi$  pathway. We, however, failed to

**TABLE 3: Total Energies (hartrees) and Relative Energies (kcal/mol) of Stationary Points on the  $X^- + \text{RCOX}$  Potential Energy Surface Calculated with the MP2/6-31+G\* Basis Set**

X	R		reactant	reactant complex	$T^-$	$E_{T^-} - E_{\text{reactant}}$	$E_{T^-} - E_{R-C}$
F	SiH <sub>3</sub>	RHF	-602.252 03		-602.298 63 I <sup>a</sup>	-29.24	
		MP2	-603.019 02		-603.070 13 I	-32.07	
		RHF	-351.225 83		-351.267 93 I	-26.42	
	CH <sub>3</sub>	MP2	-352.042 20		-352.087 15 I	-28.20	
		MP4	-352.091 56		-352.136 89	-28.44	
		RHF	-312.175 03		-312.226 03 I	-32.00	
	H	MP2	-312.861 50		-312.912 95 I	-32.28	
		MP4	-312.894 41		-312.945 61	-32.13	
		RHF					
	CN	MP2	-404.856 21		-404.941 74 I	-53.67	
		MP4	-404.905 47		-404.991 58	-54.04	
		RHF	-516.623 53		-515.738 03 I	-71.85	
NO <sub>2</sub>	MP2	-516.861 11		-516.965 68 I	-65.62		
	MP2	-1323.057 43	-1323.086 72	-1323.077 31 ( $\nu^\ddagger = 186.5 \text{ icm}^{-1}$ ) <sup>b</sup>	-12.47	5.90	
	RHF	-1071.375 75	-1071.392 09	-1071.368 23 ( $\nu^\ddagger = 98.9 \text{ icm}^{-1}$ )	4.72	14.97	
CH <sub>3</sub>	MP2	-1072.079 42	-1072.100 04	-1072.088 07 ( $\nu^\ddagger = 98.1 \text{ icm}^{-1}$ )	-5.43	7.51	
	MP4	-1072.146 89		-1072.156 70	-6.16		
	RHF	-1032.326 03	-1032.350 27	-1032.316 46 ( $\nu^\ddagger = 369.7 \text{ icm}^{-1}$ )	6.01	21.22	
H	MP2	-1032.897 70	-1032.925 95	-1032.910 13 ( $\nu^\ddagger = 92.8 \text{ icm}^{-1}$ )	-7.79	9.92	
	MP4	-1032.931 25		-1032.963 41	-8.27		
	RHF	-1124.039 65	-1124.057 59	-1124.044 64 ( $\nu^\ddagger = 161.4 \text{ icm}^{-1}$ )	-3.13	8.13	
CN	MP2	-1124.896 83		-1124.931 41 I	-21.69		
	MP4	-1124.964 39		-1124.000 18	-22.46		
	HF	-1235.776 85	-1235.799 10	-1235.794 52 I	-11.08	2.87	
NO <sub>2</sub>	MP2	-1236.906 02		-1236.953 12 I	-29.56		

<sup>a</sup> I is the intermediate, confirmed by all positive eigenvalues in the Hessian matrix. <sup>b</sup>  $\nu^\ddagger$  (i.e., TS) is confirmed by only one negative eigenvalue in the Hessian matrix.

locate such an in-plane  $\sigma$  type  $S_N2$  pathway (Table 1) at the MP2/6-311++G\*\*//MP2/6-311++G\*\* level of theory.

**(II) Effects of the Acyl Group.** The energetics for the reactions of  $\text{RCOX} + X^-$  with  $R = \text{SiH}_3, \text{CH}_3, \text{H}, \text{CN},$  and  $\text{NO}_2$  and  $X = \text{F}$  and  $\text{Cl}$  are summarized in Table 3. For  $X = \text{F}$ , all acyl groups,  $R = \text{SiH}_3, \text{CH}_3, \text{H}, \text{CN},$  and  $\text{NO}_2$ , lead to a single-well potential energy profile at both the HF and MP2 (and MP4) levels. The adduct ( $\text{RF}_2\text{CO}^-$ ) formation becomes, however, more exothermic as the acyl group,  $R$ , becomes a stronger electron acceptor, moving down the column in Table 3 (except for  $R = \text{SiH}_3$ ). In general the MP2 well-depth is greater for the relatively weak electron donors  $R = \text{SiH}_3$  and  $\text{CH}_3$ , but the trend is reversed to shallower well, for the strong acceptors,  $R = \text{CN}$  and  $\text{NO}_2$ , compared to that at the HF level. However the difference in the well-depth is very small between

the value at the MP4 level and that at the MP2 level. For  $R = \text{H}$ , the well-depth is nearly constant irrespective of the level of computation, with  $-32.0 \pm 0.1$  kcal/mol, at the HF, MP2, and MP4 levels. These could be attributed to the greater electron correlation energy in the adduct ( $E_{\text{corr}}^1$ ) than that in the initial state ( $E_{\text{corr}}^0$ ) for the weak donor ( $R = \text{SiH}_3$  and  $\text{CH}_3$ ), which should lead to a net reduction of correlated energy changes, ( $\Delta E_{\text{MP}}^1 - \Delta E_{\text{HF}}^1 < 0$ );<sup>21</sup>  $\Delta E_{\text{MP}}^1 = (E_{\text{SCF}}^1 - E_{\text{corr}}^1) - (E_{\text{SCF}}^0 - E_{\text{corr}}^0) = \Delta E_{\text{HF}}^1 - \Delta E_{\text{corr}}^1 (< \Delta E_{\text{HF}}^1)$  (Table 3). As the electron-withdrawing power of the  $R$  group increases, the electron correlation energy in the adduct is reduced and becomes less than the correlation energy in the initial state, so that the correlated energy changes ( $\Delta E_{\text{MP}}^1$ ) become greater than those at the HF level ( $\Delta E_{\text{MP}}^1 - \Delta E_{\text{HF}}^1 > 0$ ). The well-depth becomes shallower by a very small amount as the basis set used

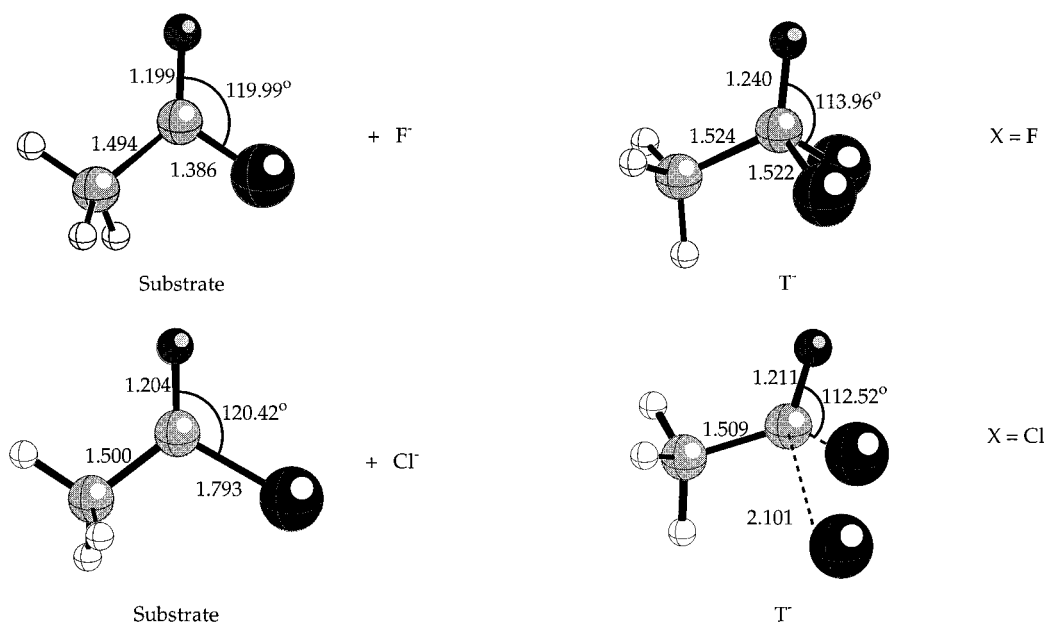


**Figure 3.** MP2 optimized structures of stationary point species for the reactions of  $X^- + \text{RCOX}$  ( $R = \text{CH}_3$ ). Distances are in angstroms and bond angles are in degrees.

in the calculations is improved; for the  $F^- + \text{HCOF}$  process, it was 31.8 kcal/mol at the MP2/6-311++G\*\*//MP2/6-311++G\*\* level in contrast to  $32.0 \pm 0.1$  kcal/mol at the MP2/6-31+G\*/MP2/6-31+G\* level. For  $X = \text{Cl}$ , however, we obtained quite an interesting result: reference to Table 3 reveals that as the acyl group becomes successively more electron-withdrawing, as indicated by the substituent electronegativity parameter,  $\sigma_X$  ( $-0.13, 0.17, 0, 0.31, \text{ and } 0.40$  for  $R = \text{SiH}_3, \text{CH}_3, \text{H, CN, and NO}_2$ , respectively),<sup>22</sup> the potential energy profile changes from a triple-well type for  $R = \text{SiH}_3, \text{CH}_3$  and  $\text{H}$  to a single-well type for  $R = \text{CN}$  and  $\text{NO}_2$ . Moreover for the former series the central (intrinsic) barrier,  $\Delta E_0^\ddagger$ , increases from 5.9 to 7.5 and to 9.9 kcal/mol at the MP2 level as  $R$  is changed from  $\text{SiH}_3$  to  $\text{CH}_3$  and to  $\text{H}$ . For the latter series, the well-depth increases from  $-21.7$  to  $-29.6$  kcal/mol at the MP2 level as  $R$  becomes a stronger electron acceptor from  $\text{CN}$  to  $\text{NO}_2$ . The adduct is stabilized slightly more at the MP4 than at the MP2 level. At the HF level, the triple-well potential energy profiles are obtained even for the electron acceptors with a decrease in the central barrier height as the  $R$  group becomes a stronger acceptor. This is in contrast to the single-well potential energy profiles obtained at the MP2 level with a deeper well-depth as the electron-accepting power of  $R$  increases. The change of mechanism from a triple-well type to a single-well type is therefore strongly dependent on the electron-withdrawing power of the acyl group. The triple-well type obtained at the HF level for  $R = \text{CN}$  and  $\text{NO}_2$  is again an artifact of the neglect of electron correlation effect. The MP2 optimized structures for some ( $R = \text{CH}_3$ ) of the stationary point species are presented in Figure 3. The triple-well potential energy profiles obtained for  $\text{Cl}^- + \text{HCOCl}$  and  $\text{Cl}^- + \text{CH}_3\text{COCl}$  reactions at both the HF and MP2 levels are in agreement with the experimental results of Brauman and co-workers<sup>48</sup> and also with the *ab initio* results at lower levels than our work; our MP2 central (intrinsic) barriers,  $\Delta E_0^\ddagger$ , for the two reactions are 5.9 ( $R = \text{H}$ ) and 9.9 kcal/mol ( $R = \text{CH}_3$ ). Our  $\Delta E_0^\ddagger$  value for  $R = \text{H}$  is lower than those at the MP2/6-31+G\*\*//3-21+G (11.7 kcal/mol)<sup>8</sup> and MP3/MP2/6-31+G\*\*//3-21+G (15.3 kcal/mol) levels.<sup>8</sup> Our  $\Delta E_0^\ddagger$  value for  $R = \text{CH}_3$  is lower than that with HF/4-31G\*\*//4-31G\*\* (14.2 kcal/mol)<sup>9</sup> but is higher than that with HF/3-21+G//3-21+G basis set (7.5 kcal/mol).<sup>8</sup> Those  $\Delta E_0^\ddagger$  values obtained without electron correlation effect are, however, unreliable.

In summary, factors that favor formation of a stable adduct with a single-well potential energy profile can be summarized as follows: (a) The stronger the nucleophilicity and the weaker the nucleofugacity, the more the stable adduct formation is favored. Since the electronegativity of the radical and anionic forms of  $X$  increases in the order  $\text{H}^- < \text{F}^- < \text{Cl}^-$ , the stable adduct formation will be favored in the reverse order; the nucleophilicity is in the reverse order, whereas the nucleofugacity is in the same order as the order of increasing electronegativity. (b) The stronger the  $\text{C}-X$  bond, the greater the possibility of adduct formation. The  $\text{C}-X$  bond strength is in the order (in kcal/mol)  $\text{C}-\text{Cl}$  (79)  $<$   $\text{C}-\text{H}$  (99)  $<$   $\text{C}-\text{F}$  (116).<sup>16</sup> This predicts that the adduct will be more stable with  $X = \text{F}$  than with  $X = \text{H}$ , in contrast to the reverse order found in this work showing that the bond strength requirement is not the only, or predominant, factor. (c) The wider the energy gap between the two antibonding orbitals,  $\sigma_{\text{C}-X}^*$  and  $\pi_{\text{C}=\text{O}}^*$ , the more the adduct formation favored; this is due to the difficulty of mixing-in the  $\sigma_{\text{C}-X}^*$  orbital to the initially attacked  $\pi_{\text{C}=\text{O}}^*$ , which leads to tetrahedral adduct formation. The mixing of the two MOs,  $\pi_{\text{C}=\text{O}}^*$  and  $\sigma_{\text{C}-\text{Cl}}^*$ , transforms the latter,  $\sigma_{\text{C}-\text{Cl}}^*$ , as a main component of the LUMO so that the tetrahedral species becomes a transition state due to facile bond cleavage of the  $\text{C}-\text{Cl}$  bond. The energy gaps are indeed large (7–9 au) for  $X = \text{F}$  with all the  $R$  groups, so that adduct formation takes place with  $X = \text{F}$ . In contrast for  $X = \text{Cl}$ , the energy gap increases

gradually from ca. 3 to 5 au as  $R$  is varied from  $\text{SiH}_3$  to  $\text{NO}_2$ . For  $R = \text{CN}$  and  $\text{NO}_2$  the energy gaps are relatively large, so that for these two compounds the single-well potential energy profile with a stable adduct prevails in contrast to the other three,  $R = \text{SiH}_3, \text{CH}_3$ , and  $\text{H}$ , for which the triple-well energy profiles are obtained due to efficient orbital mixing between  $\pi_{\text{C}=\text{O}}^*$  and  $\sigma_{\text{C}-\text{Cl}}^*$ .

**Acknowledgment.** We thank the Korea Research Center for Theoretical Physics and Chemistry and Inha University for support of this work.

## References and Notes

- (1) Determination of Reactivity by MO Theory, Part 98. For part 97, see: Lee I.; Koh H. J.; Chang, B. D. *Bull. Korean Chem. Soc.* **1995**, *16*, 1104.
- (2) (a) Bender, M. L. *Chem. Rev.* **1960**, *60*, 53. (b) Patai, S., Ed. *The Chemistry of Carbonyl Group*; Interscience: New York, 1966, 1970; Vols. 1, 2. (c) Jencks, W. P. *Acc. Chem. Res.* **1980**, *13*, 161.
- (3) (a) Ba-Saif, S.; Luthra, A. K.; Williams, A. *J. Am. Chem. Soc.* **1987**, *109*, 6362. (b) Henge, A. *J. Am. Chem. Soc.* **1992**, *114*, 6575. (c) Williams, A. *Chem. Soc. Rev.* **1994**, *93*. (d) Williams, A. *Acc. Chem. Res.* **1989**, *22*, 387.
- (4) (a) Tiedemann, P. W.; Riveros, J. M. *J. Am. Chem. Soc.* **1974**, *96*, 185. (b) McMahon, T. B. *Can. J. Chem.* **1978**, *56*, 670. (c) Pau, J. K.; Kim, J. K.; Caserio, M. C. *J. Am. Chem. Soc.* **1978**, *100*, 3831. (d) Kim, J. K.; Caserio, M. C. *J. Am. Chem. Soc.* **1981**, *103*, 2124. (e) Fukuda, E. K.; McIver, R. T., Jr. *J. Am. Chem. Soc.* **1979**, *101*, 2498. (f) Comisarow, M. *Can. J. Chem.* **1977**, *55*, 171. (g) Asubiojo, O. I.; Brauman, J. I. *J. Am. Chem. Soc.* **1979**, *101*, 3715. (h) Olmstead, W. N.; Brauman, J. I. *J. Am. Chem. Soc.* **1977**, *99*, 4219. (i) Bowie, J. H.; Williams, B. D. *Aust. J. Chem.* **1974**, *27*, 1923. (j) Bowie, J. H. *Acc. Chem. Res.* **1980**, *13*, 76. (k) McDonald, R. N.; Chowdhury, A. K. *J. Am. Chem. Soc.* **1983**, *105*, 7267. (l) McDonald, R. N.; Chowdhury, A. K. *J. Am. Chem. Soc.* **1983**, *105*, 198. (m) Larson, J. W.; McMahon, T. B. *J. Phys. Chem.* **1984**, *88*, 1083. (n) Klass, G.; Skeldon, J. C.; Bowie, J. H. *J. Chem. Soc., Perkin Trans. 2* **1983**, 1337. (o) Han, C. C.; Brauman, J. I. *J. Am. Chem. Soc.* **1990**, *112*, 7835. (p) Wilbur, J. L.; Brauman, J. I. *J. Am. Chem. Soc.* **1994**, *116*, 5839.
- (5) (a) Burgi, H. B.; Lehn, J. M.; Wipff, G. *J. Am. Chem. Soc.* **1974**, *96*, 1956. (b) Burgi, H. B.; Dunitz, J. D.; Lehn, J. M.; Wipff, G. *Tetrahedron* **1974**, *30*, 1563.
- (6) Tanner, S. D.; Mackay, G. I.; Bohme, D. K. *Can. J. Chem.* **1981**, *59*, 1615.
- (7) Madura, J. D.; Jorgensen, W. L. *J. Am. Chem. Soc.* **1986**, *108*, 2517.
- (8) Blake, J. F.; Jorgensen, W. L. *J. Am. Chem. Soc.* **1987**, *109*, 3856.
- (9) (a) Yamabe, S.; Minato, T. *J. Org. Chem.* **1983**, *48*, 2972. (b) Yamabe, S.; Minato, T.; Kawabata, Y. *Can. J. Chem.* **1984**, *62*, 235.
- (10) Frish, M. J.; Trucks, G. W.; Head-Gordon, M.; Gill, P. M. W.; Wong, M. W.; Foresman, J. B.; Johnson, B. G.; Schlegel, H. B.; Robb, M. A.; Replogle, E. S.; Gomperts, R.; Andres, J. L.; Raghavachari, K.; Binkley, J. S.; Gonzalez, C.; Martin, R. L.; Fox, D. J.; Defrees, D. J.; Baker, J.; Stewart, J. J. P.; Pople, J. A. *Gaussian 92*, Revision A; Gaussian Inc.: Pittsburgh, PA, 1992.
- (11) Hehre, W. J.; Radom, L.; Schleyer, P. v. R.; Pople, J. A. *Ab Initio Molecular Orbital Theory*; Wiley: New York, 1986; Chapter 6.
- (12) Csiszmadia, I. G. *Theory and Practice of MO Calculation on Organic Molecules*; Elsevier: Amsterdam, 1976; p 239.
- (13) Kebarle, P.; Chowdhury, S. *Chem. Rev.* **1987**, *87*, 513.
- (14) Baer, S.; Brinkman, E. A.; Brauman, J. I. *J. Am. Chem. Soc.* **1991**, *113*, 805.
- (15) Wu, Y.-D.; Houk, K. N. Unpublished work cited in ref 6.
- (16) Klumpp, G. W. *Reactivity in Organic Chemistry*; Wiley: New York, 1982; p 38.
- (17) (a) Pearson, R. G. *J. Org. Chem.* **1989**, *54*, 1423. (b) Pearson, R. G. *J. Chem. Educ.* **1987**, *64*, 561.
- (18) Park, Y. S.; Kim, C. K.; Lee, B.-S.; Lee, I. *J. Phys. Chem.* **1995**, *99*, 13103.
- (19) Yamabe, S.; Koyama, T.; Minato, T.; Inagaki, S. *Bull. Chem. Soc. Jpn.* **1990**, *63*, 1684.
- (20) Glukhovtsev, M. N.; Pross, A.; Radom, L. *J. Am. Chem. Soc.* **1994**, *116*, 5961.
- (21) Lee, I.; Kim, C. K.; Chung, D. S.; Lee, B.-S. *J. Org. Chem.* **1994**, *59*, 4490.
- (22) The  $\sigma_X$  scale is defined by  $1 - q_{\text{H}}$  for the proton in molecules  $\text{HX}$  as obtained at the 6-31G\*\*//6-31G\* level. The  $\sigma_X$  value is considered to represent group electronegativity of  $X$  in molecules  $\text{HX}$ . Thus if the group  $X$  is more electronegative,  $\sigma_X$  becomes more positive. (a) Reynolds, W. F.; Taft, R. W.; Topsom, R. D. *Tetrahedron Lett.* **1982**, 1055. (b) Marriott, S.; Reynolds, W. F.; Taft, R. W.; Topsom, R. D. *J. Org. Chem.* **1984**, *49*, 959.